

# Detecting low-level flexibility using residual dipolar couplings. A study of the conformation of cellobiose

## Supporting Information

Nicholle G. A. Bell,<sup>a</sup> Graeme Rigg,<sup>a</sup> Sarah Masters,<sup>b</sup> Juraj Bella<sup>a</sup> and Dušan Uhrín<sup>a\*</sup>

<sup>a</sup> EastChem School of Chemistry, University of Edinburgh, West Mains Road, Edinburgh, EH9 3JJ, UK.

<sup>b</sup> Now Department of Chemistry, University of Canterbury, Private Bag 4800, Christchurch 8140, New Zealand.

Sample preparation details, definition of the order parameter and calculations of rmsds

Figure 1S. 800 MHz <sup>13</sup>C spectrum of cellobiose.

Figure 2S. Illustration of the measurement of homonuclear splittings.

Figure 3S. 2D INADEQUATE spectra of cellobiose in aligned media.

Figure 4S. 2D contour plot of the rmsds between the experimental and theoretical RDCs as a function of  $\phi_r$ ,  $\psi_r$  angles.

Figure 5S. 2D contour plot of the rmsds between the experimental and theoretical inter-glycosidic  $J$  couplings of  $\alpha$ -D-cellobiose as a function of  $\phi_r$ ,  $\psi_r$  angles.

Figure 6S. 2D contour plot of the rmsds between the experimental and theoretical RDCs +  $J$  couplings as a function of  $\phi_r$ ,  $\psi_r$  angles.

Figure 7S. Relationship between the  $\phi_H$  and  $\psi_H$  angles in twenty-one X-ray structures of cellobiose related oligosaccharides.

**Sample preparation details.** The procedure to optimise the alignment media was as follows. Initially, the C12E5 was dissolved in the D2O and mixing thoroughly. Hexanol was then added in 5  $\mu$ l proportions via a careful pipetting technique, vortexing well after each addition. The ternary mixture, initially appeared biphasic, and upon further addition of the hexanol turned visually opalescent and viscous in nature, indicating that the lyotropic liquid crystalline phase was achieved. The composition of the final mixture had molar ratio of C12E5 to hexanol of 0.95 and a C<sub>12</sub>E<sub>5</sub>/D<sub>2</sub>O ratio of 9.8 wt %. To ensure the media was homogenous and bubble free, the sample was centrifuged and later heated in the NMR spectrometer to 313 K. The alignment was quantified by measuring the residual quadrupolar splitting of the deuterium signal of D<sub>2</sub>O. Cellobiose was then added to the alignment media, and the sample was centrifuged. The sample, once homogenised and cooled, was found to have deuterium splitting of 44 Hz at 298 K. Temperature insensitive CD3 resonances of acetone-d<sub>6</sub>, contained within a capillary inserted into a regular NMR tube, were used for deuterium lock and shimming. This arrangement also enabled the use of autoshim on aligned samples, which would otherwise not be possible due to the residual quadrupolar coupling of D<sub>2</sub>O.

**Definitions.** The parameters of the order matrix (eigenvectors and eigenvalues) were determined using home-written SVD program. The generalised order parameter (GDO) was determined using Eqn. 3:

$$G = D = \frac{\sqrt{2}}{\sqrt{3}} \sum_{ij} S_{ij}^2 \quad (3)$$

where  $S_{ij}$  are the Saupe order matrix elements. The parameter  $\eta$ , which is proportional to the rhombicity of the alignment, was calculated using Eqn. 4.

$$\eta = \frac{S_{xx} - S_{yy}}{S_{zz}} \quad (4)$$

The theoretical RDCs determined by the SVD method were compared with the experimental ones and the average pairwise rmsd were calculated. In addition, RDCs were also analysed using the software REDCAT.<sup>1</sup>

The rmsds between the experimental and theoretical  ${}^3J_{CH}$  couplings related to the geometry of the glycosidic linkage were calculated using Eqn. 5:

$$rmsd({}^3J(\phi_H, \psi_H)) = \sqrt{0.5 * (({}^3J_{H1',C4}^{exp} - {}^3J_{H1',C4}^{calc})^2 + ({}^3J_{C2',C4}^{exp} - {}^3J_{C2',C4}^{calc})^2) + 0.333 * (({}^3J_{C1',H4}^{exp} - {}^3J_{C1',H4}^{calc})^2 + ({}^3J_{C1',C3}^{exp} - {}^3J_{C1',C3}^{calc})^2 - ({}^3J_{C1',C5}^{exp} - {}^3J_{C1',C5}^{calc})^2)} \quad (5),$$

where  ${}^3J_{CH}^{calc}$  were calculated<sup>2</sup> using Eqn. 6

$${}^3J_{CH}^{calc} = 5.7 \cos^2 \alpha - 0.6 \cos^2 \alpha + 0.5, \quad \alpha = \psi_H, \phi_H \quad (6)$$

${}^3J_{C2',C4}^{calc}$  ( ${}^3J_{C1',C3}^{calc}$ ) were calculated<sup>3</sup> using Eqn. 7

$${}^3J_{C2',C4}^{calc} ({}^3J_{C1',C3}^{calc}) = 3.49 \cos^2(\varphi_H + 120) + 0.16 \quad (7)$$

${}^3J_{C1',C5}^{calc}$  were calculated<sup>3</sup> using Eqn. 8

$${}^3J_{C1',C5}^{calc} = 3.49 \cos^2(\psi_H - 120) + 0.16 \quad (8)$$

while the combined  $J$  and RDC rmsds were calculated using Eqn. 9.

$$rmsd(RDC, {}^3J(\phi, \psi)) = rmsd(RDC(\phi, \psi)) + rmsd({}^3J(\phi, \psi)) \quad (9)$$

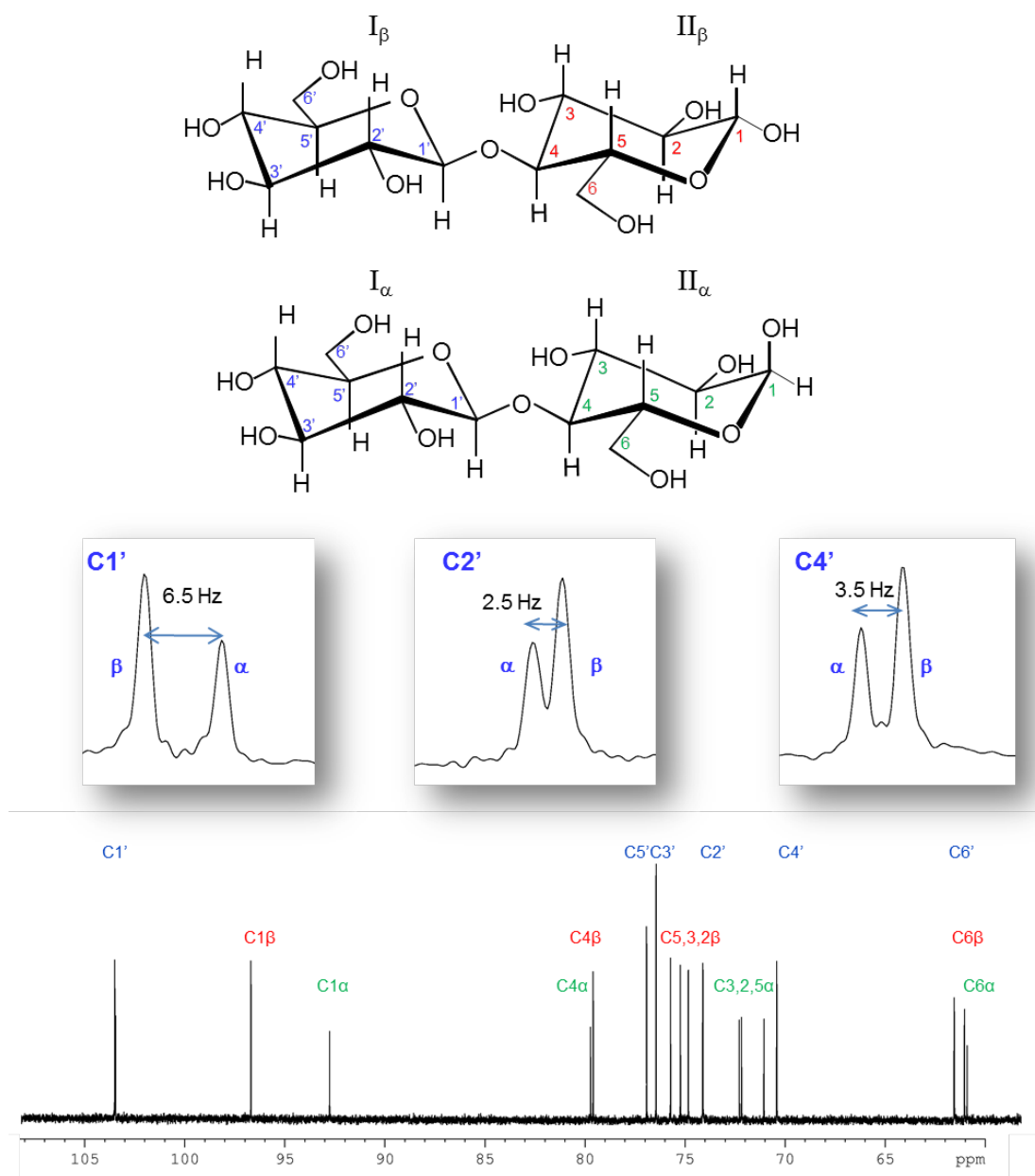


Figure 1S. 800 MHz  ${}^{13}\text{C}$  spectrum of cellobiose. The insets show the cellobiose structures and expansions containing closely resonating  ${}^{13}\text{C}$  signals of the non-reducing rings,  $\text{I}_\alpha$  and  $\text{I}_\beta$ .

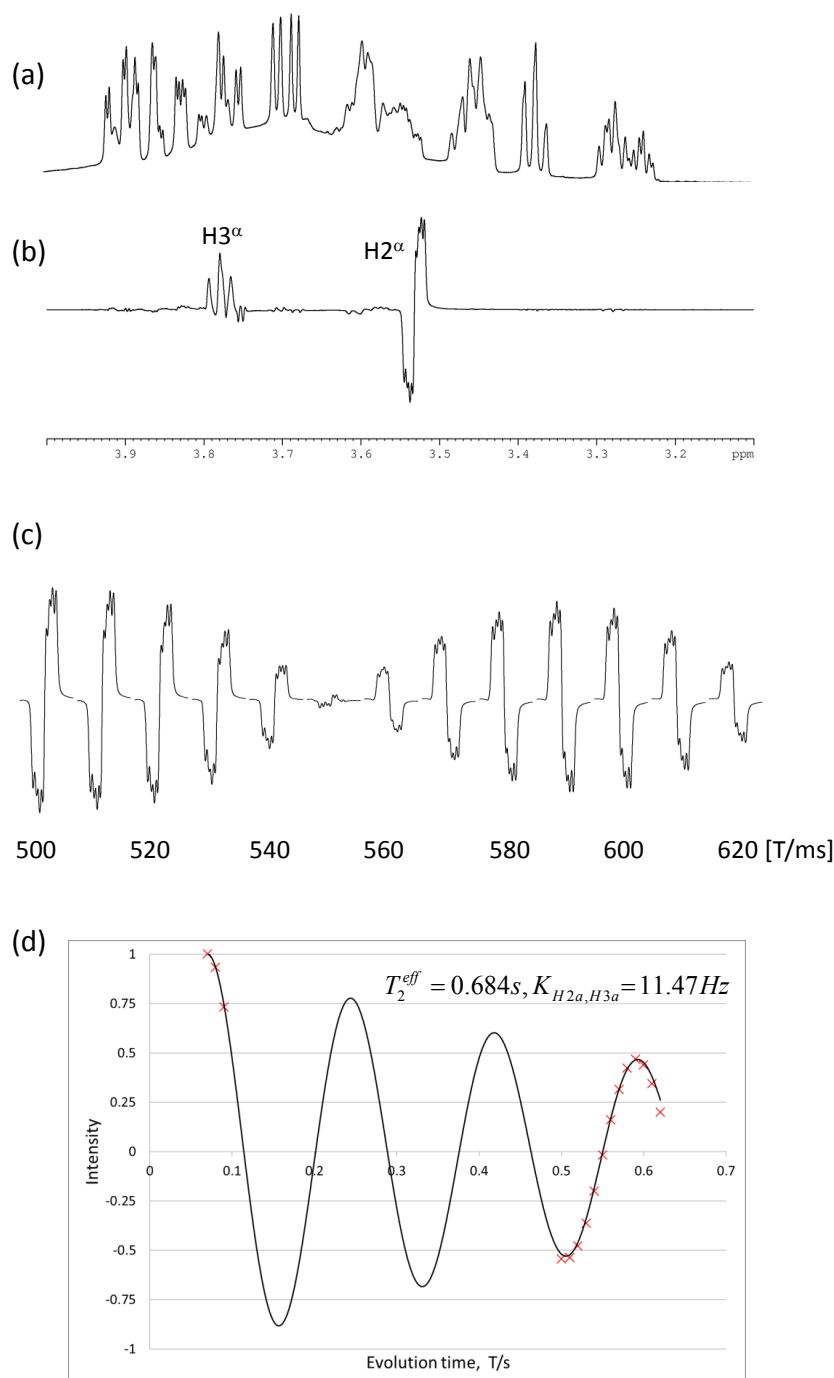


Figure 2S. (a) Partial 800 MHz  $^1\text{H}$  NMR spectrum of aligned cellobiose. Note that the cellobiose signals are superimposed on a broad signal of the aligning medium. (b) A  $J$ -modulated 1D directed CSSF-COSY spectrum<sup>4</sup> with the selection of  $\text{H3}^\alpha$  and the transfer of magnetisation to  $\text{H2}^\alpha$ . A 30 ms Gaussian pulse was used during the CSSF; a 30 ms  $\text{H3}^\alpha / \text{H2}^\alpha$  double selective Gaussian pulse was applied in the middle of the evolution interval  $T$ . Two scans were acquired in each of 20 increments of the CSSF. The length of one increment of the CSSF was set to 5 ms. (c) Signal of  $\text{H2}^\alpha$  as a function of the evolution time,  $T$ . (d) Experimental ( $\times$ ) and theoretical (Eqn. 2, the main text) intensities of  $\text{H2}^\alpha$  shown in (c). Few points are acquired using short evolution times, while the majority data points are timed later on. This allows for proper fitting of the relaxation time and improves the accuracy of the determined splitting.

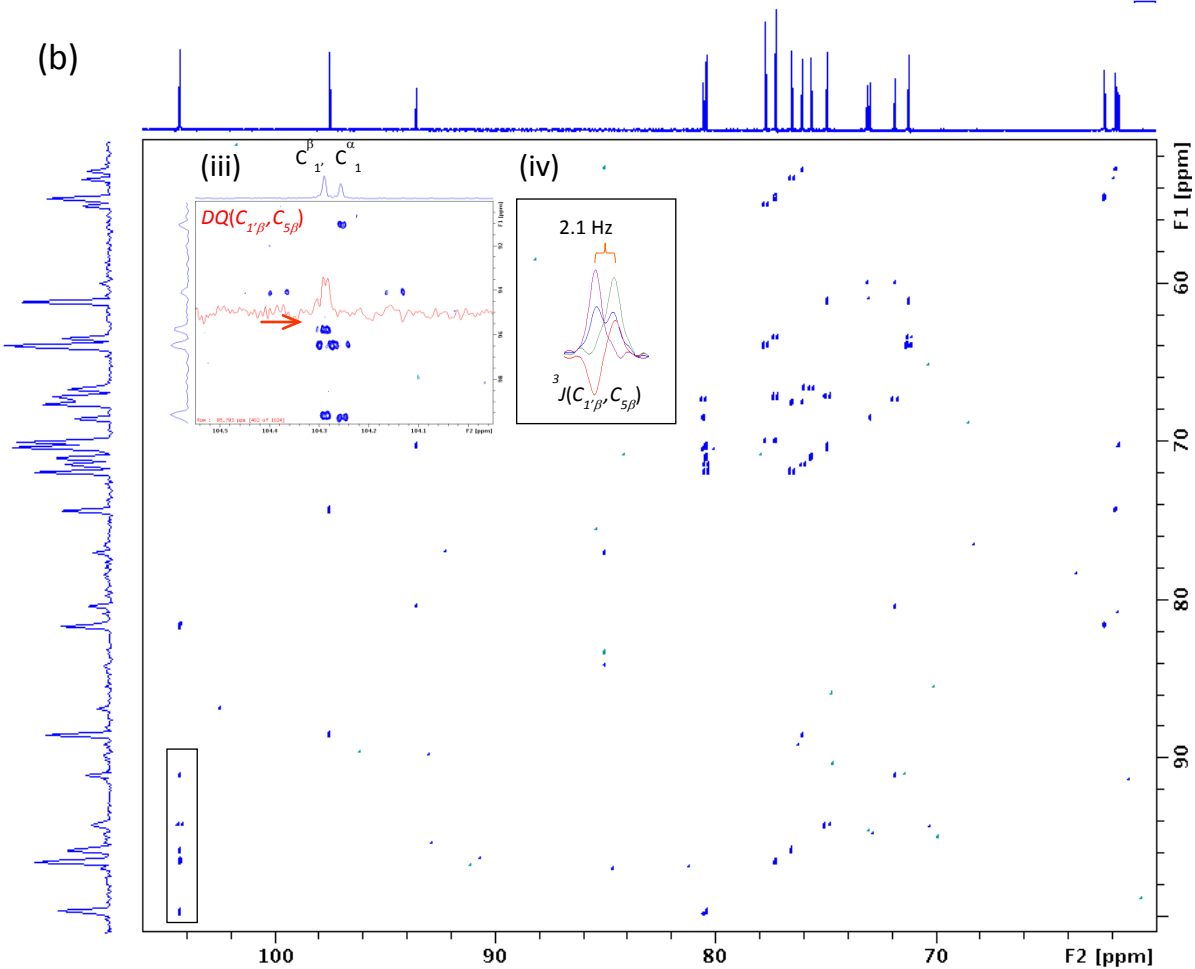
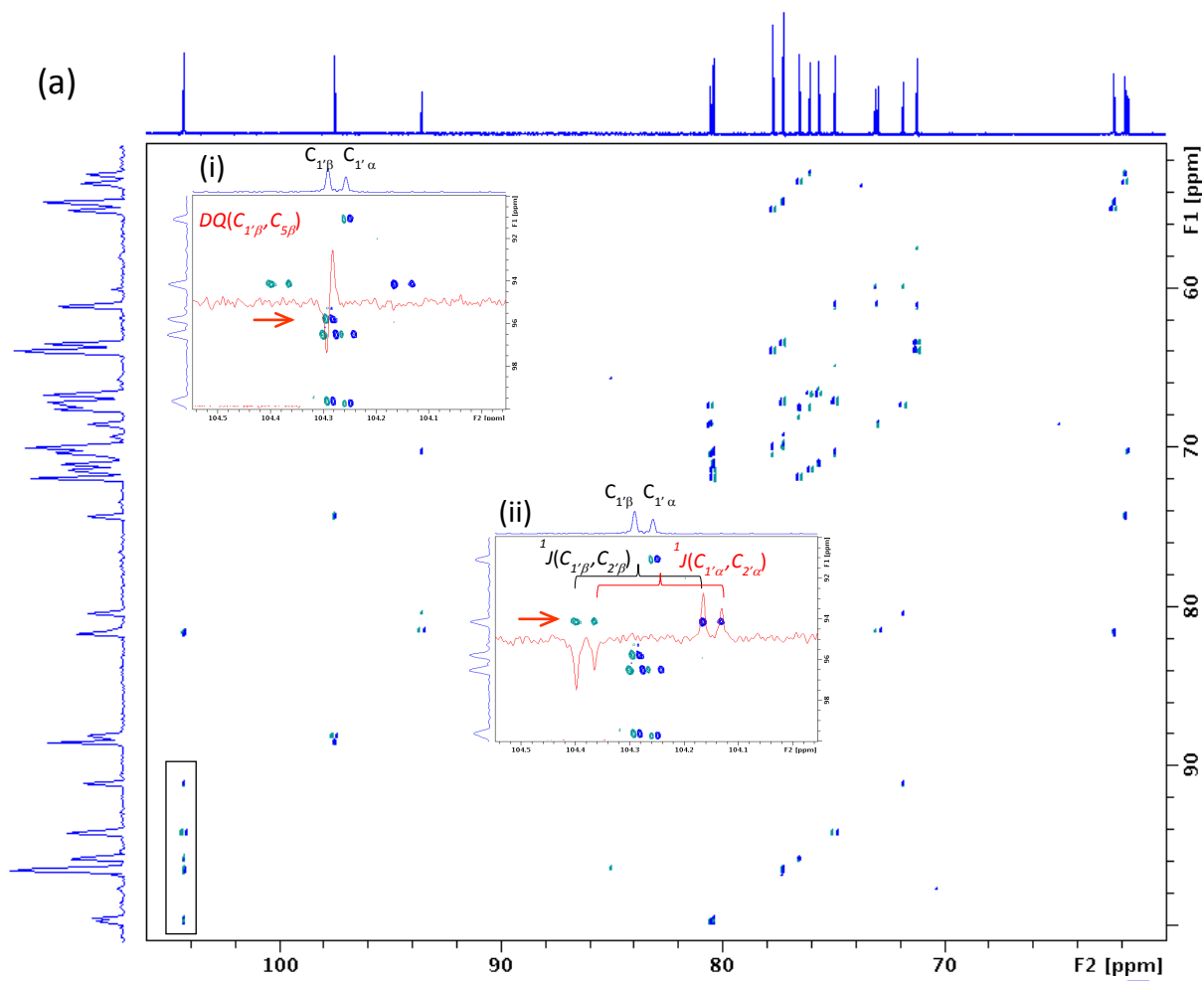


Figure 3S. 2D INADEQUATE<sup>5</sup> spectra of cellobiose in the aligned medium. (a) the anti-phase and (b) in-phase 2D spectra were acquired in an interleaved manner using the following parameters: number of scans 128 per  $t_1$  increment, acquisition times  $t_1 = 10.6$  ms and  $t_2 = 0.682$  s, relaxation time of 0.5 s. The evolution of anti-phase magnetisation ( $1/2^n J_{CC}$ ) was optimised for  ${}^n J_{CC} = 3.76$  Hz. This setting ensured that cross peaks due to  ${}^1 J_{CC}$  coupling appeared with good intensities and variation of the evolution interval was not invoked. The total acquisition time for both spectra was 50 hours. The insets (i) – (iii) show expansions of the areas enclosed in the black rectangles together with rows taken at the DQ frequencies indicated with a red arrow. The inset (iv) shows editing of the in-phase (blue) and anti-phase (red) long-range cross-peaks of the  $C_{1\beta}$ ,  $C_{5\beta}$  DQ coherence yielding single lines of a doublet (green, violet).

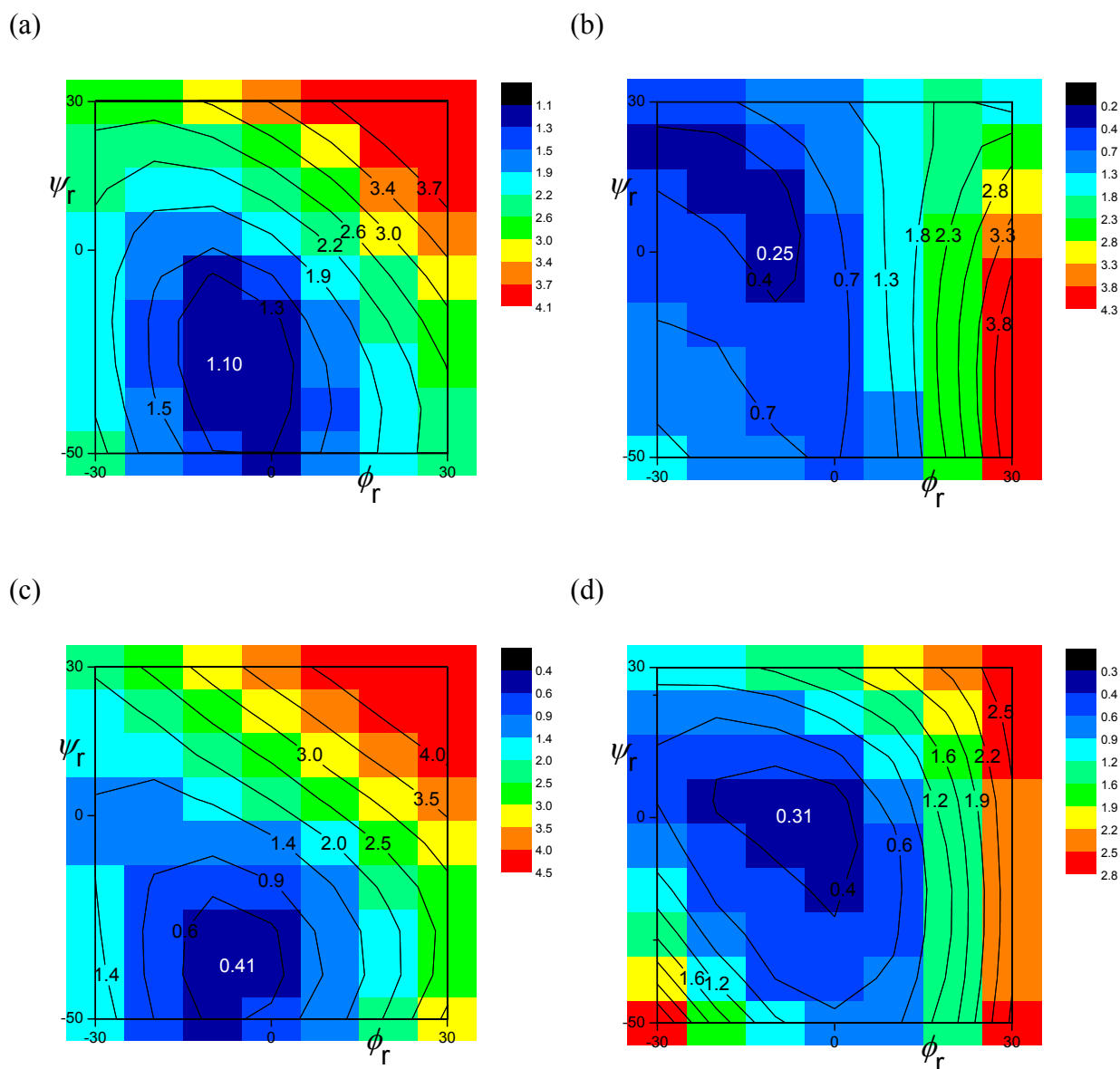


Figure 4S. 2D contour plot of the rmsds between the experimental and theoretical RDCs as a function of  $\phi_r$ ,  $\psi_r$  angles. (a)  $\alpha$ - D-cellobiose, the rmsds of ring II were based on the alignment of ring I. The global minimum has coordinates ( $\phi_r/^\circ$ ,  $\psi_r/^\circ$ , rmsd/Hz) = (-10, -30, 1.10); (b)  $\alpha$ - D-cellobiose, the rmsds of ring I were based on the alignment of ring II. The global minimum has coordinates ( $\phi_r/^\circ$ ,  $\psi_r/^\circ$ , rmsd/Hz) = (-10, 0, 0.25); (c)  $\beta$ - D-cellobiose, the

rmsds of ring **II** were based on the alignment of ring **I**. The global minimum has coordinates  $(\phi_r/^\circ, \psi_r/^\circ, \text{rmsd/Hz}) = (-10, -40, 0.41)$ ; (d)  $\beta$ -D-cellobiose, the rmsds of ring **I** were based on the alignment of ring **II**. The global minimum has coordinates  $(\phi_r/^\circ, \psi_r/^\circ, \text{rmsd/Hz}) = (-10, 0, 0.31)$ .

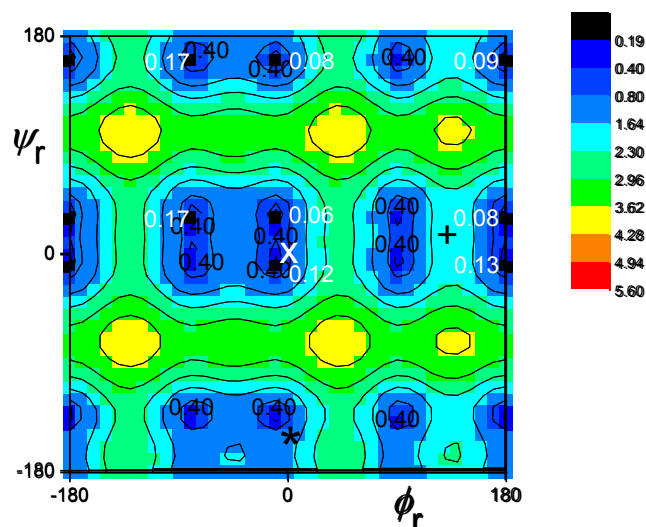


Figure 5S. The rmsds between the experimental and theoretical  $^3J_{\text{CH}}$  and  $^3J_{\text{CC}}$  coupling constants of  $\alpha$ -D-cellobiose (Table 2) as a function of  $\phi_r, \psi_r$  angles. The position of conformers identified by molecular mechanics calculations<sup>6</sup> is indicated by \* ( $\text{syn}\phi_{\text{H}}/\text{anti}\psi_{\text{H}}$ ) and + ( $\text{anti}\phi_{\text{H}}/\text{syn}\psi_{\text{H}}$ ), while the (0,0) coordinates indicating the  $\phi_r$  and  $\psi_r$  of the X-rays structure of cellobiose<sup>7</sup> is identified by a white X.

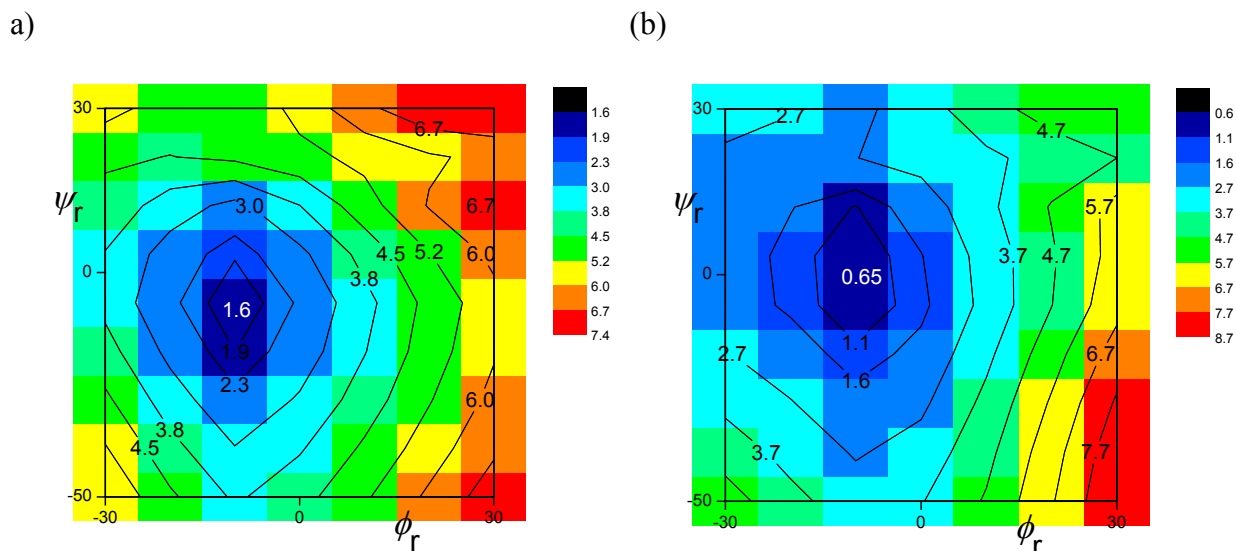


Figure 6S.2D contour plot of the rmsds between the experimental and theoretical RDCs and  $J$  couplings of  $\alpha$ -D-cellobiose as a function of  $\phi_r, \psi_r$  angles. (a) the rmsds of ring **II** were based on the alignment of ring **I**. The global minimum has coordinates  $(\phi_r/^\circ, \psi_r/^\circ, \text{rmsd/Hz}) = (-10, -10, 1.6)$ ; (b) the rmsds of ring **I** were based on the alignment of ring **II**. The global minimum has coordinates  $(\phi_r/^\circ, \psi_r/^\circ, \text{rmsd/Hz}) = (-10, 0, 0.65)$ .

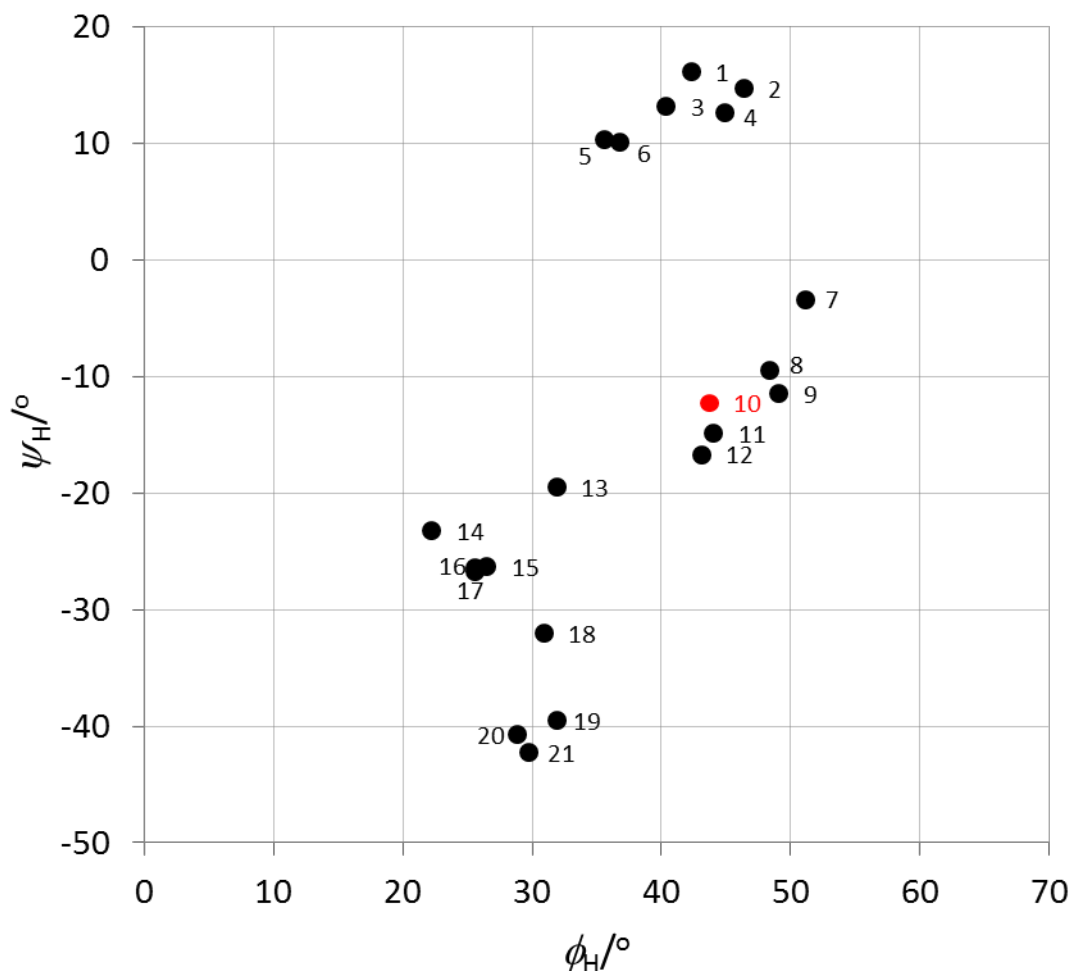


Figure 7S. Relationship between the  $\phi_H$  and  $\psi_H$  angles of twenty-one X-ray structures of cellobiose (red circle) and related oligosaccharides<sup>8</sup> (black circles). 1. Cellobiose octaacetate; 2. Cellobiose·2 NaI·2 H<sub>2</sub>O; 3. *N,N'*-Diacetylchitobiosamine; 4. Cellotriose undecaacetate ('nonreducing'); 5. 6'-*O*-Trityl- $\alpha$ -D-cellobiose heptaacetate; 6. 4-*O*- $\beta$ -D-Galactosyl- $\alpha$ -D-mannose; 7. Methyl hepta-*O*-nitro- $\beta$ -cellobioside; 8. Methyl 6,6'-dinitro- $\beta$ -cellobioside; 9.  $\beta$ -Lactose; 10.  $\beta$ -D-Cellobiose; 11. Lactose CaBr<sub>2</sub>·7 H<sub>2</sub>O; 12. Lactose CaCl<sub>2</sub>·7 H<sub>2</sub>O; 13. *N*-Acetyl lactosamine·H<sub>2</sub>O; 14. Cellotriose acetate ('reducing'); 15.  $\alpha$ -Lactose; 16. Methyl cellotrioside (average of 8); 17. Cellotetraose (average of 6); 18. Methyl 4-*O*-methyl- $\beta$ -D-glucosyl- $\beta$ -D-glucose; 19. Lactosylurea·2 H<sub>2</sub>O; 20. Methyl- $\beta$ -cellobioside MeOH; 21. *N,N'*-Diacetyl- $\beta$ -chitobiose·3 H<sub>2</sub>O.

- (1) Valafar, H.; Prestegard, J. H. *Journal of Magnetic Resonance* **2004**, *167*, 228.
- (2) Tvaroska, I.; Hricovini, M.; Petrakova, E. *Carbohydrate Research* **1989**, *189*, 359.
- (3) Bose, B.; Zhao, S.; Stenutz, R.; Cloran, F.; Bondo, P. B.; Bondo, G.; Hertz, B.; Carmichael, I.; Serianni, A. S. *Journal of the American Chemical Society* **1998**, *120*, 11158.
- (4) Jin, L.; Pham, T. N.; Uhrin, D. *Chemphyschem* **2007**, *8*, 1228.
- (5) Jin, L.; Uhrin, D. *Magnetic Resonance in Chemistry* **2007**, *45*, 628.
- (6) Peric-Hassler, L.; Hansen, H. S.; Baron, R.; Hunenberger, P. H. *Carbohydrate Research* **2010**, *345*, 1781.
- (7) Chu, S. S. C.; Jeffrey, G. A. *Acta Crystallographica Section B-Structural Crystallography and Crystal Chemistry* **1968**, *B 24*, 830.
- (8) Peralta-Inga, Z.; Johnson, G. P.; Dowd, M. K.; Rendleman, J. A.; Stevens, E. D.; French, A. D. *Carbohydrate Research* **2002**, *337*, 851.